ISSN 0015-4628, Fluid Dynamics, 2024, Vol. 59, No. 4, pp. 639–652. © Pleiades Publishing, Ltd., 2024.

Absolute and Global Instability of Plane Submerged Jets

V. V. Vedeneev[a],*, L. R. Gareev[a],, Ju. S. Zayko[a],***, and N. M. Exter[a],******

[a] *Moscow State University, Institute of Mechanics, Moscow, Russia*

**e-mail: vasily@vedeneev.ru*

***e-mail: gareev@imec.msu.ru*

****e-mail: zayko@imec.msu.ru*

*****e-mail: exter@imec.msu.ru*

Received April 5, 2024; revised June 10, 2024; accepted July 11, 2024

Abstract—The family of velocity profiles of a submerged jet, which are absolutely unstable in the plane-parallel approximation, is considered. The profiles are specified by two parameters: the first of them is responsible for the location of the only inflection point in the velocity profile, and the second is responsible for the shear layer thickness. An algorithm for determining the length of the region of local absolute instability of the jet with a given input velocity profile, that is, the distance at which absolute instability gives way to convective instability, has been implemented. The dependence of this length on the parameters defining the input profile is obtained. A connection between the characteristics of local absolute instability calculated in the plane-parallel approximation and global instability of the jet evolving in space is analytically obtained. The input velocity profile that corresponds to sufficiently large length of the zone of local absolute instability, at which global instability of spatially developing jet occurs, is demonstrated. Thus, the possibility of existence of global instability of plane submerged jets with special velocity distributions is demonstrated.

Keywords: jet flow, linear stability theory, absolute instability, global instability

DOI: 10.1134/S0015462824603346

A jet that flows out into a medium with the same aggregate state as the jet itself is called a submerged jet. Such jets are often encountered in science and technology, and their loss of stability and transition to turbulence significantly affects such phenomena as combustion, mixing, chemical reactions, and sputtering. The stability of jet flows can depend on various factors, for example, the flow velocity, the density, the viscosity, and the temperature of the jet and surrounding fluid, etc. Under certain specific conditions, jet flows can be laminar over large distances downstream [1–4], while under the normal conditions they lose stability and become turbulent over distances of 1–2 widths/diameters of outlet cross-section. Control of submerged jets and prediction of their loss of stability are of interest in the context of fundamental and applied problems.

Instability of a plane-parallel fluid flow can be of two types: convective and absolute. In the case of convective instability, small disturbances are carried away with time, grow downstream, and, reaching a certain level, lead to turbulence transition. In this case, the achievement of a significant amplitude of disturbances and turbulence transition often occur much downstream from the place of origin of the growing disturbance. As a consequence, such a flow may have the laminar region of large length [5]. Examples of convectively unstable flows are the plane-parallel Poiseuille flow [6, 7] and the Blasius boundary layer [8]. In the case of absolute instability, the disturbance grows unboundedly with time at the point in space (in flow) where it appears.

The submerged jets with the classic velocity profiles and the density not different from the density of the surrounding medium can be absolutely unstable only in the presence of a counterflow on the boundary [9]. However, for the jets with complex "non-classical" profiles, it was found that absolute instability without counterflow is possible for both the round [10] and plane [11] jets.

Owing to the spatial evolution of unperturbed flow, the existence of global eigenmodes, i.e., time-harmonic disturbances localized in space (which is impossible in plane-parallel flows) becomes possible. More strictly, by eigenmodes we will mean the disturbances that satisfy zero conditions in the inlet jet cross-section and at infinite distance from the jet in all directions, and depend on time as $e^{-i\omega t}$. If any

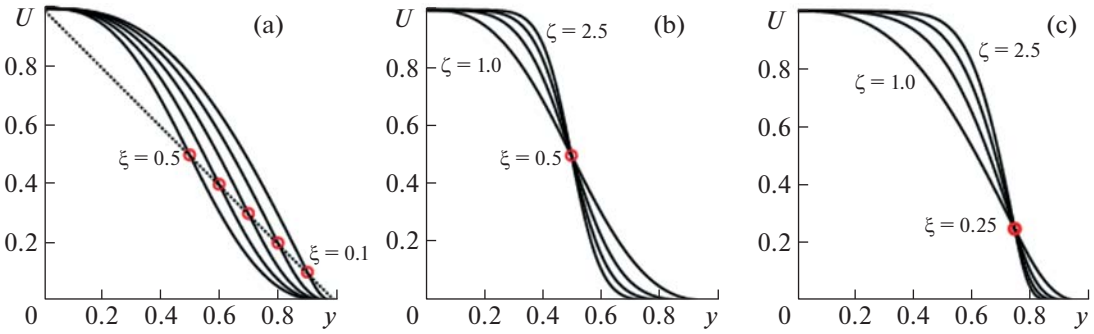

Fig. 1. Velocity profiles specified by the pair of parameters ξ, ζ: $\xi \le 0.5$, $\zeta = 1$ (a), $\xi = 0.5$, $\zeta \ge 1$ (b), and $\xi = 0.25$, $\zeta \ge 1$ (c). Red circle denotes the inflection point.

eigenmode is growing in time, then the region of its localization is a zone of generation of self-excited oscillations. We will call the existence of growing eigenmodes by global instability [12, 13], where the term "global" emphasizes non-local (non-plane-parallel) stability analysis. An interest in creating globally unstable flows is due to the fact that areas of self-excitation of oscillations in their nonlinear development can lead to the development of regular secondary or chaotic turbulent flows, which can be used in the designing of various devices and technologies to intensify mixing.

It is well known [12, 13] that in evolving flows with the presence of two spatial waves (that is, described by the second-order dispersion equation in the wavenumber), for existence of a growing global eigenmode, the presence of a zone of local absolute instability is necessary. The global instability of flow, which is caused by local absolute instability, explains a number of phenomena: the appearance of the Kármán street in the wake of a cylinder [14, 15], oscillations and destruction of hot jets [16], oscillations of the wake of wing airfoils [17], disintegration of liquid jets into drops [18, 19], and axisymmetric motions of a non-Newtonian liquid in inhomogeneous elastic tubes [20].

However, this condition is not sufficient: for growing global oscillations to develop, in the general case, the zone of local absolute instability must be sufficiently extended, and the growth rate must be sufficiently large. Otherwise, the surrounding zone of convective instability will "outweigh" the absolute instability: the disturbances arising in the zone of absolute instability will partially leave it and be carried downstream, which will prevent the growth of such disturbances in the generation zone. As a result, all global eigenmodes will be damped, that is, there will be no zones of generation of self-excited oscillations in flow, and the introduced growing disturbances will be carried downstream.

In the present work, the length of the region of local absolute instability of a plane submerged jet is determined. Section 1 provides the mathematical formulation of the problem and gives the brief description of the algorithm for determining the length of the region of local absolute instability. Section 2 is devoted to detailed description of the algorithm. Section 3 describes the results of calculations for the considered family of velocity profiles. In Section 4 the characteristics of the zone of local absolute instability, leading to global instability of a spatially evolving jet are defined; an example of parameters under which global instability can be expected is given.

1. FORMULATION OF THE PROBLEM

We will pose the problem, whose aim is to develop an algorithm for determining the lengths of local absolute instability regions of plane unidirectional jets, specified by the initial velocity profiles introduced in [11] and determined by two parameters ξ, ζ. The parameter ξ is responsible for the location of the inflection point in the velocity profile; the parameter ζ determines the width of the shear layer of the jet (Fig. 1). The axis x lies in the plane of flow and is directed downstream, the y axis is perpendicular to it and lies in the plane of flow.

Initially, we will numerically simulate steady-state flow and calculate the downstream evolution of the initial jet velocity profile specified by a pair of parameters ξ, ζ. Then, we will analyze the type of instability of the velocity profiles at various distances from the beginning of the jet by searching for saddle points on the complex wave number plane ($\mathrm{Re}\alpha$, $\mathrm{Im}\alpha$). Thus, we search for the length of the local absolute instability region of a particular jet, determined by the parameters ξ, ζ of the initial velocity profile. The term

"local" is used in the sense that the analysis of the nature of instability is carried out in the plane-parallel approximation without taking into account modification of the velocity profile along the coordinate x.

The study and the results are presented in dimensionless form; the maximum velocity U_{max} and half the width of the jet $h/2$ are taken as the linear scales of the velocity and the length, respectively. Using these parameters, the Reynolds number of the flow $R = 9000$ is also calculated. This value of R was taken based on experiments carried out on a facility that creates a laminar plane air jet of thickness $h = 0.1$ m with the maximum velocity on the jet axis $U_{max} = 2.78$ m/s. Based on the results of ongoing theoretical work, it is planned to conduct experiments on this facility on creating globally unstable flow.

The instability is studied in the inviscid approximation since the jets are analyzed at the Reynolds numbers that can be considered to be farly high for the following reason. In [11], a plane-parallel analysis of instability was carried out with account for viscosity and critical Reynolds numbers which separate the convective and absolute instability zones. The results of the theoretical analysis were confirmed by direct numerical simulation. The characteristic critical Reynolds numbers are of the order of 1000, i.e., they are an order lower than those considered in the present study. This justifies the use of inviscid stability theory.

Thus, the algorithm consists of the following stages:

(1) parameterization of the initial velocity profile: choice of a pair of the parameters ξ, ζ;

(2) laminar time-independent calculation of the jet with a given initial velocity profile;

(3) processing of numerical calculation results: recording the velocity profiles at various distances downstream;

(4) analysis of the type of instability (convective/absolute) of these velocity profiles;

(5) determination of the distance at which absolute instability gives way to convective instability.

What follows is a detailed description of each stage.

2. DESCRIPTION OF THE ALGORITHM FOR DETERMINING THE LENGTH OF THE REGION OF LOCAL ABSOLUTE INSTABILITY

2.1. Family of the Velocity Profiles under Study

Setting the initial profile by the parameters ξ, ζ was carried out using fifth-degree splines, in accordance with how it was done in [11]. Initially, we will consider the case $\zeta = 1$:

$$\tilde{U}_s(y) = \begin{cases} f(y), & 0 \le y \le y_0; \quad f(y) = a_5 y^5 + a_4 y^4 + a_3 y^3 + 1 \\ g(y), & y_0 \le y \le 1, \quad g(y) = b_5 (y-1)^5 + b_4 (y-1)^4 + b_3 (y-1)^3. \end{cases} \tag{2.1}$$

The velocity profile under study has a single inflection point at a given point $y = y_0 = 1 - \xi$. The polynomials of this type must satisfy the boundary conditions:

$$f(0) = 1, \quad f'(0) = f''(0) = 0, \quad g(1) = g'(1) = g''(1) = 0.$$

To determine the coefficients of polynomials, the smoothness conditions are set at the point of gluing the polynomials:

$$f(y_0) = g(y_0), \quad f'(y_0) = g'(y_0), \quad f''(y_0) = g''(y_0),$$

there are also three following conditions at the inflection point:

$$f(y_0) = \xi, \quad f'(y_0) = -2, \quad f''(y_0) = 0.$$

Thus, ξ is the control parameter of the inflection point of the velocity profile: it is located at the point $y_0 = 1 - \xi$, and the velocity at the inflection point is $U(y_0) = \xi$. In Fig. 1a we have plotted the resulting graphs.

The effect of the second parameter ζ at $\zeta > 1$ is to increase the velocity gradient at the inflection point by reducing the thickness of the shear layer of the jet, as shown in Fig. 1b. It occurs due to transformation of the coordinate y. We will define the following spline function of the fifth degree on $\tilde{y}(y)$ in the segment $0 \le y \le 1$:

$$\tilde{y}(y) = \begin{cases} \phi(y), & 0 \le y < y_0 \\ \psi(y), & y_0 < y \le 1, \end{cases}$$

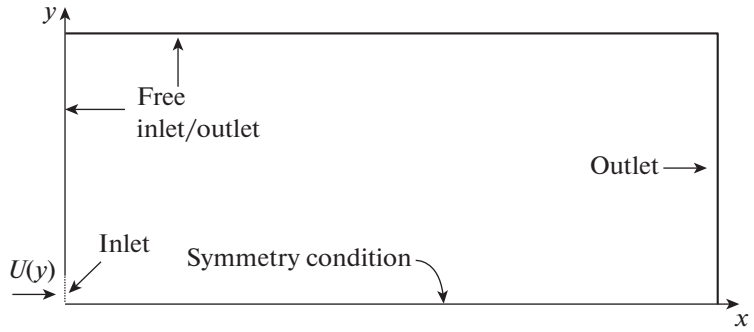

Fig. 2. Computational domain for the symmetrical half of a plane unidirectional submerged jet.

which satisfies the following conditions:

$$\tilde{y}(0) = 0, \quad \tilde{y}(y_0) = y_0, \quad \tilde{y}(1) = 1;$$
$$\tilde{y}'(0) = \nu, \quad \tilde{y}'(y_0) = \zeta, \quad \tilde{y}'(1) = \nu;$$
$$\tilde{y}''(0) = 0, \quad \tilde{y}''(y_0) = 0, \quad \tilde{y}''(1) = 0;$$

where y_0 is the inflection point of the velocity profile, $\zeta \geq 1$ is the control parameter, and $\nu = 1/\zeta^2$. After transforming the coordinates, the velocity profile takes the form:

$$U(y) = U_s(\tilde{y}(y)),$$

where U_s is the initial spline-defined velocity profile (2.1).

The resulting profile is controlled by both parameters: ξ sets the location of the inflection point, and $\zeta \geq 1$ determines the thickness of the shear layer (Fig. 1c).

2.2. Steady-State Flow Calculations

The laminar stationary calculation is carried out in the CFD complex with a given initial velocity profile. The system of Navier–Stokes equations is solved by the control volume method implemented in the Ansys CFX solver. The computational domain is shown in Fig. 2. It represents a symmetric half of the jet and the region of the surrounding space, since the problem of the plane flow of a unidirectional jet is solved. As a boundary condition at the inlet (dashed curve in Fig. 2), a streamwise velocity profile is specified — the velocity distribution along the coordinate y. At the outlet, the atmospheric pressure is specified, on the upper and left boundaries of the computational domain we have the free inlet/outlet, namely, the zero normal gradient of the velocity direction and the atmospheric pressure, on the lower boundary — the symmetry condition. The length of the calculation area is equal to 25 and the height is equal to 10.

To simulate plane flow, the three-dimensional model with a single layer of elements in the transverse direction and the symmetry conditions on the side surfaces were considered. Hexahedral elements, whose total number was equal to 272 130 (470 × 579 elements along the x and y axes) were used; within the main jet flow, the grid became denser, it contained 188 000 (470 × 400) elements. The calculations were carried out using a first-order spatial upwind scheme using the establishing method until the level of the maximum dimensionless discrepancy for all elements was reduced to 10^{-6}. For all calculations described below, convergence in the grid and the size of the computational domain has been achieved.

2.3. Processing of CFD Calculation Results. Analysis of the Type of Instability of the Velocity Profiles in a Jet at Various Distances from its Beginning

After completing the CFD calculation, the streamwise velocity profiles are taken at various distances from the beginning of the jet downstream with a step $\Delta x = x_{i+1} - x_i = 0.2$. Here $i = 0,\ldots,N$, where N is the number of the first velocity profile, whose type of instability will be convective. For each of the velocity profiles, linear instability is analyzed in the inviscid approximation. A plane-parallel approach in which

$u_x = U(y)$ and $u_y = u_z = 0$ is used. The perturbations in the form of traveling waves are superimposed on the unperturbed motion

$$\begin{pmatrix} u'_x \\ u'_y \\ u'_z \end{pmatrix} = \begin{pmatrix} U'_x(y) \\ U'_y(y) \\ U'_z(y) \end{pmatrix} e^{i(\alpha x - \omega t)}. \tag{2.2}$$

The system of Navier–Stokes equations is linearized about the unperturbed state, taking into account the fact that the Reynolds number of the flow under consideration is large: R = 9000, that is, we can assume that $R \to \infty$. Thus, we obtain the Rayleigh equation for the disturbance component $U'_y = \psi(y)$:

$$(U(y) - c)\left(\frac{d^2\psi}{dy^2} - \alpha^2\psi\right) - \frac{d^2U}{dy^2}\psi = 0. \tag{2.3}$$

Here, $c = \omega/\alpha$ is the phase velocity, ω is the frequency, and α is the wavenumber. For the symmetric velocity profile, the quantities $\psi(y)$ are always even and odd functions of y. The boundary conditions have the following form:

$$\frac{d\psi}{dy} = 0 \quad \text{at} \quad y = 0 \quad \text{for the odd eigenfunction,} \tag{2.4}$$

$$\psi = 0 \quad \text{at} \quad y = 0 \quad \text{for the even eigenfunction,} \tag{2.5}$$

$$\frac{d\psi}{dy} + \alpha\psi = 0 \quad \text{at} \quad y = \delta. \tag{2.6}$$

We will explain the derivation of condition (2.6). It is assumed that outside the jet the medium is at rest: $U(y) = 0$ at $y \geq \delta$. The general solution of the Rayleigh equation, which is the second-order differential equation with constant coefficients in this domain, takes the form $\psi = C_1 e^{\alpha y} + C_2 e^{-\alpha y}$ ($C_1, C_2 = \text{const}$, $\alpha \geq 0$), and, since the disturbances decay as $y \to \infty$, we have $C_1 = 0$. To merge the disturbance in the external flow with the disturbance in the jet at $y = \delta$ it is necessary that $d\psi/dy|_{y=\delta} = -\alpha\psi$.

Equation (2.3) with boundary conditions (2.4)–(2.6) represent the eigenvalue problem $\alpha(\omega) \in \mathbb{C}$ at a given frequency $\omega \in \mathbb{R}$ (that is, those α are sought for which the problem has a non-zero solution). For each fixed α integration (2.3) from 0 to δ is carried out by the Runge-Kutta method with initial conditions (2.4) and $\psi(0) = 1$, or (2.5) and $d\psi/dy(0) = 1$. Then the expression

$$\Psi(\alpha) = \frac{d\psi}{dy}(\delta) + \alpha\psi(\delta),$$

is calculated and, using the secant method, we seek the zero of the function

$$\Psi(\alpha) = 0.$$

In our calculations, $\delta = 1.2$ was adopted, since for all the velocity profiles considered below with high accuracy $U(y) \approx 0$ at $y > \delta$.

Note that in the case of neutral perturbations ($\text{Im}\alpha = 0$), the Rayleigh equation has a singularity lying on the path of integration along the y axis [22]. However, this singularity disappears in the case of growing disturbances. Therefore, the results for neutral perturbations given below were obtained as the limit of growing perturbations at the growth rate tending to zero, i.e., as $\text{Im}\,\alpha \to -0$. This limitation could be avoided by taking the integration path that bypasses the singularity in the complex plane y, as was done in [21]; however, such an approach was not used in this study, since the nature of instability is determined by the saddle point lying in the domain $\text{Im}\alpha < 0$ in which this problem does not exist.

In the general case, the solution to the problem with initial data on the propagation of a localized disturbance contains components of both a discrete and a continuous spectrum [22]. In the problem considered here, there is a single growing mode $\omega(\alpha)$ from the discrete spectrum, whose behavior determines the

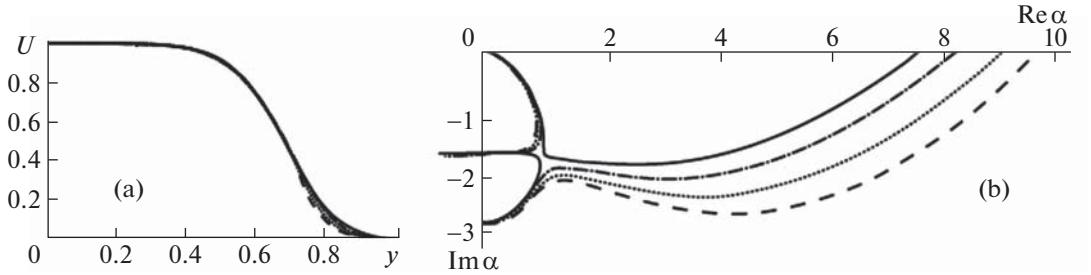

Fig. 3. Velocity profiles (a) and the corresponding level lines $\mathrm{Im}\omega = 0$ in the plane $\alpha \in \mathbb{C}$ for a jet with the parameters $\xi = 0.25$ and $\zeta = 2$; (b) dashed curves correspond to the velocity profiles and level lines at $x = 1$, dotted at $x = 2$, dash-and-dot at $x = 4$, and solid at $x = 6.6$.

asymptotic (as $t \to \infty$) behavior of the perturbation $w(x, y, t)$ (here, w is any of the components of velocity perturbation); therefore, it can be written in the form of the Fourier integral:

$$w(x, y, t) = \int_{-\infty}^{\infty} f(\alpha, y) e^{i(\alpha x - \omega(\alpha) t)} d\alpha. \tag{2.7}$$

The type of instability, i.e., the tendency of $w(x, y, t)$ to 0 or ∞ as $t \to \infty$, is determined by the saddle point method [22] and reduces to analyzing the behavior of level lines $\mathrm{Im}\,\omega = 0$ in the plane $\alpha \in \mathbb{C}$. For the family of velocity profiles under consideration, there is a saddle point (α_s, ω_s) in this plane, through which the integration contour for the Fourier integral (2.7) can uniquely be drawn [10]. Note that as $\mathrm{Re}\,\alpha \to \pm\infty$, the integration path coincides with the straight line $\mathrm{Im}\alpha = 0$, when $\mathrm{Im}\omega(\alpha) < 0$. In this case, the asymptotic behavior of the Fourier integral is determined by the value of the quantity $\mathrm{Im}\omega_s = \mathrm{Im}\omega(\alpha_s)$ at the saddle point α_s in the plane $\alpha \in \mathbb{C}$ and, according to the saddle point method, takes the following form:

$$w(x, y, t) \sim e^{i\theta} f(\alpha_s, y) \sqrt{\frac{2\pi}{|\omega''(\alpha_s)|}} \frac{e^{i(\alpha_s x - \omega_s t)}}{\sqrt{t}}, \tag{2.8}$$

where $\theta \in \mathbb{R}$. In the case of absolute instability at the saddle point we have $\mathrm{Im}\omega_s > 0$, while in the case of convective instability $\mathrm{Im}\omega_s < 0$.

As an example, for a jet with the initial velocity profile determined by the parameters $\xi = 0.25, \zeta = 2$, in Fig. 3a we have plotted the velocity profiles at the distances $x = 1, 2, 4$ and 6.6. In Fig. 3b the constructed level lines $\mathrm{Im}\,\omega = 0$ for $x = 1, 2$ and 4 correspond to the case of absolute instability. In these cases, the integration path and the directions of increase and decrease in $\mathrm{Im}\omega$ in the vicinity of the saddle point are shown in Fig. 4a: the value of $\mathrm{Im}\omega$ is positive at the saddle point. In the case of convective instability ($x = 6.6$, solid curves in Fig. 3b), one of the level lines $\mathrm{Im}\,\omega = 0$ continuously connects two neutral disturbances, and the directions of increase and decrease in $\mathrm{Im}\omega$ in the vicinity of the saddle point are such that the value of $\mathrm{Im}\omega$ at the saddle point turns out to be negative (Fig. 4b). Thus, in the case of convective instability, one of the branches continuously connects two neutral disturbances, and the sign of $\mathrm{Im}\omega$ is negative at the saddle point. Similarly, by analyzing the location of level lines in the complex wavenumber plane, the type of instability is determined for each profile considered for each of the calculated jets. The automated analysis was performed as follows:

(1) The above-described eigenvalue problem $\alpha(\omega) \in \mathbb{C}$ is solved at real frequencies $\omega \in (0; \omega_{\mathrm{neutr}}]$. The calculations start with $\omega = \omega_{\mathrm{neutr}}$ with subsequent decrease in ω. The result is the right-hand level line $\mathrm{Im}\,\omega = 0$ (Fig. 3b) in form of a two-dimensional array of values of $\mathrm{Re}\alpha$ and $\mathrm{Im}\alpha$.

(2) The left part of this level line (after passing through the vicinity of the saddle point with decrease in ω) determines the nature of instability. To do this, an array of differences $\mathrm{Im}\alpha_{i+1} - \mathrm{Im}\alpha_i$ is calculated from the array $\mathrm{Im}\alpha$. Based on the predominance of negative or positive numbers in it, it is concluded whether the level line goes down or up after passing the vicinity of the saddle point. In the first case, the instability is absolute (Fig. 4a), in the second - convective (Fig. 4b).

(3) Steps 1–2 are carried out for slices of the velocity profiles, whose initial form is determined by the pair (ξ, ζ), with a step $\Delta x = 0.2$ until the nature of instability changes from absolute to convective. Thus,

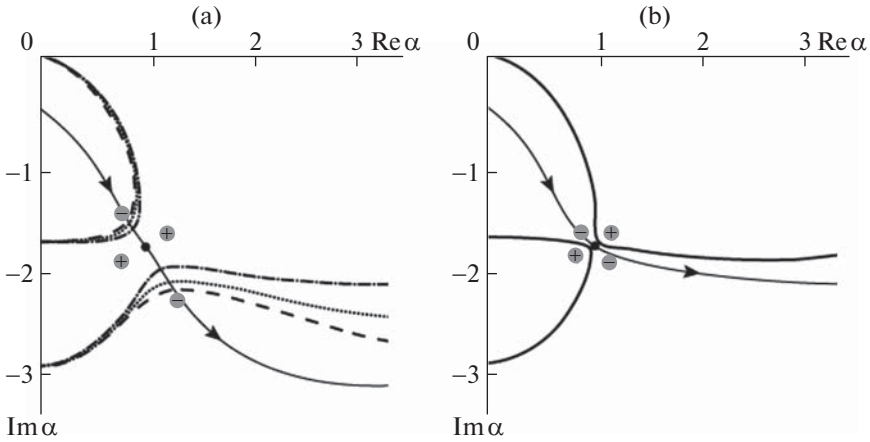

Fig. 4. Level lines $\mathrm{Im}\omega = 0$ in the plane $\alpha \in \mathbb{C}$ in the cases of absolute (a) and convective (b) instability for the jet velocity profiles at various distances from the beginning. Black dot denotes the vicinity of the saddle point. Signs "±" in gray circles show the directions of decrease and increase in the vicinity of the saddle point. Thin curve with arrows shows the integration path. The type of curves corresponds to Fig. 3.

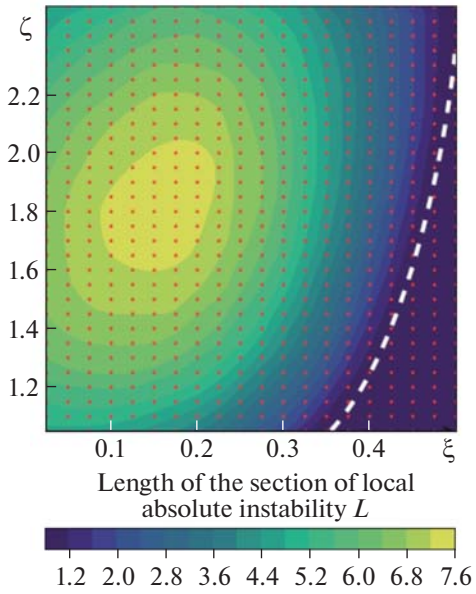

Fig. 5. Length of the region of local absolute instability as a function of the parameters ξ, ζ. Red dots denote the considered velocity profiles.

for each pair (ξ, ζ), the downstream coordinate $x = L$ is calculated, which determines the length of the region of local absolute instability.

3. RESULTS OF CALCULATION OF LOCAL ABSOLUTE INSTABILITY OF JETS

Using the algorithm developed, an analysis of 600 jet velocity profiles specified by various pairs (ξ, ζ) was carried out. The parameter ξ varied in the range [0.025; 0.5] with a step 0.025 and the parameter ζ varied in the range [1.05; 2.5] with a step 0.05. The results of calculating the length of the local absolute instability region are shown in Fig. 5. Dark blue color in the fill indicates the absence of the region of local absolute instability, yellow color indicates the area in the ξ, ζ plane with the greatest length obtained. For the longest region we have $L \approx 7.6$.

In [11], for the range of parameters $\xi \in [0.34, 0.5]$, $\zeta \in [1, 2.4]$ (without taking into account the evolution of the jet profile downstream), the boundary of absolute and convective instabilities was found, i.e., a curve above which the velocity profiles are absolutely unstable and below which they are convectively unstable. In Fig. 5, this curve is shown by a white dashed line. It can be seen that in the fill obtained in this work, in the region below the dashed line there are no areas of local absolute instability of the jets. Thus, this result is in agreement with the data from [11].

4. GLOBAL INSTABILITY OF A JET EVOLVING DOWNSTREAM

Above, a local analysis of instability of the jet flow, which does not take into account the spatial "blurring" of the velocity profile, was carried out. Then, taking into account this "blurring," the global instability of flow under consideration is studied based on the construction and analysis of a model equation that reflects the main properties of the original flow. Namely, the global eigenmode arises as a consequence of local absolute instability [12, 13], and that, in turn, is explained by the merging of two wavenumbers $\alpha(\omega)$ at the saddle point, one of the wavenumbers corresponding to a wave moving upstream, the other to a wave moving downstream [22] (the direction of the wave is determined by sign of $\mathrm{Im}\alpha$ as $\mathrm{Im}\,\omega \to +\infty$). Then it is natural to assume that the two waves determine the presence of global instability. We will consider the dispersion equation with the coefficients depending on x, which reproduces, when its coefficients "are frozen" at various distances downstream, the vicinity of the saddle point of the function $\omega(\alpha)$, which determines the nature of instability of the jet. Using this dispersion equation, we can reconstruct the corresponding differential equation with variable coefficients. In what follows, based on the exact solution of this equation, we will obtain a criterion that relates the frequency of the global eigenmode to the characteristics of local absolute instability.

4.1. Model Equation That Describes Local Absolute Instability

Following [23], we will consider the linearized Ginzburg-Landau equation for a certain unknown function $A(x,t)$ (for example, it may be one of the components of the velocity disturbance), that describes two spatial waves, and, therefore, has the second order in x:

$$\frac{\partial A}{\partial t} + u_0(x)\frac{\partial A}{\partial x} = \varkappa(x)\frac{\partial^2 A}{\partial x^2} + \mu(x)A, \tag{4.1}$$

where u_0, $\varkappa$, and μ are, in the general case, complex-valued and dependent-on-x functions. To choose these functions such that they can reproduce the behavior of spatial waves in the vicinity of the saddle point of the jet, we first study the local properties of the model equation.

For this purpose, we will freeze the coefficients of the equation and consider the solutions in the form of traveling waves $A(x,t) = e^{i(\alpha x - \omega t)}$. Substitution in (4.1) leads to the local dispersion equation

$$-i\omega + iu_0\alpha = -\varkappa\alpha^2 + \mu.$$

This equation can be written in the form:

$$(\alpha - \alpha_s)^2 = \lambda(\omega - \omega_s) \Rightarrow \alpha_{1,2} = \alpha_s \pm \sqrt{\lambda(\omega - \omega_s)}, \tag{4.2}$$

where

$$\alpha_s = -\frac{iu_0}{2\varkappa}, \quad \omega_s = -i\frac{u_0^2}{4\varkappa} + i\mu, \quad \lambda = \frac{i}{\varkappa}. \tag{4.3}$$

It is obvious that the frequency $\omega = \omega_s$ is the branch point of the complex function $\alpha(\omega)$, that is, two spatial waves corresponding to two wave numbers $\alpha(\omega)$ merge at it. This point is the saddle point of the inverse function $\omega(\alpha)$, which, by definition, can be sought as a solution to the equation $d\omega/d\alpha = 0$ [24]. The parameters α_s and ω_s determine the location of the interaction point, and the parameter $\lambda = (\alpha - \alpha_s)^2/(\omega - \omega_s)$ determines the rotation ($\mathrm{Arg}\lambda$) and scaling ($|\lambda|$) of the neighborhood of the saddle point.

To "emulate" the saddle point obtained from solving the problem of hydrodynamic stability for a jet, we will take the parameters of Eq. (4.2) α_s, ω_s, and λ so that the pattern observed in the jet would be reproduced. Solving system (4.3), we find:

$$\varkappa = \frac{i}{\lambda}, \quad u_0 = -2\frac{\alpha_s}{\lambda}, \quad \mu = -i\omega_s + \frac{u_0^2}{4\varkappa} = -i\omega_s - i\frac{\alpha_s^2}{\lambda}.$$

As calculations of the evolution of the jet show (see Section 4.3), when the velocity profile blurs, the location of the saddle point, as well as the location of the branches in this plane (that is, the parameter λ), varies only slightly. The frequency $\mathrm{Re}\omega_s$ also remains close to a constant. However, the absolute instability growth rate decreases with the distance from the inlet jet cross-section, and its decrease occurs close to a linear law with increase in the distance from the initial jet cross-section: $\mathrm{Im}\,\omega_s(x) \approx a - bx$, $b > 0$. Taking into account all of the above, we obtain that

$$\varkappa \approx \mathrm{const}, \quad u_0 \approx \mathrm{const}, \quad \mu(x) \approx \mu_0 - \mu_1 x, \tag{4.4}$$

where

$$\mu_1 = b = -\frac{d\mathrm{Im}\omega_s(x)}{dx} \in \mathbb{R}. \tag{4.5}$$

Thus, the model equation that describes variation in the local properties of the flow downstream, close to the jet, takes the form:

$$\frac{\partial A}{\partial t} + u_0\frac{\partial A}{\partial x} = \varkappa\frac{\partial^2 A}{\partial x^2} + (\mu_0 - \mu_1 x)A. \tag{4.6}$$

4.2. Eigenmodes of the Model Equation

We will consider the eigenmodes of the resulting equation, that is, the solutions that depend harmonically on time and satisfy zero boundary conditions in the initial jet cross-section and when moving away from it downstream:

$$A(x,t) = e^{-i\omega t}B(x), \quad B(0) = 0, \quad B(+\infty) = 0.$$

We obtain the eigenvalue problem for the equation

$$\varkappa\frac{d^2B(x)}{dx^2} - u_0\frac{dB(x)}{dx} + \left(\mu_0 - \mu_1 x + i\omega\right)B(x) = 0.$$

The resulting equation can be reduced to the Airy equation by simple transformations. Namely, we will make the change $B(x) = e^{i\alpha_s x}C(x)$, where $\alpha_s = -iu_0/(2\varkappa)$, and the change of the variable x by a new variable z:

$$x = \left(\frac{\varkappa}{\mu_1}\right)^{1/3} z + x_0, \quad x_0 = \frac{\mu_0 - \dfrac{u_0^2}{4\varkappa} + i\omega}{\mu_1}. \tag{4.7}$$

We obtain the Airy equation

$$\frac{\partial^2 C(z)}{\partial z^2} - zC(z) = 0$$

with the boundary conditions

$$C(z) = 0 \quad \text{at} \quad z = -\frac{x_0}{(\varkappa/\mu_1)^{1/3}} \quad \text{and} \quad z \to +\infty.$$

We restrict our attention to the case

$$-\pi/3 < \mathrm{Arg}(\varkappa/\mu_1)^{1/3} < \pi/3, \tag{4.8}$$

then the tendency of the function to zero along the real axis x is equivalent (due to the properties of the Airy equation) to such a tendency along the real axis z.

The solution to the Airy equation that satisfies the second boundary condition—the downstream attenuation condition—is the Airy function $C(z) = Ai(z)$. Satisfying the first boundary condition, namely, the condition of the absence of disturbance in the initial section, we obtain

$$-\frac{x_0}{(\varkappa/\mu_1)^{1/3}} = \zeta_n \Rightarrow x_0 = -\zeta_n\left(\frac{\varkappa}{\mu_1}\right)^{1/3},$$

where ζ_n are zeros of the Airy function (real negative numbers). From here, using (4.7), we obtain the spectrum of global natural frequencies ω^g

$$\omega_n^g = i\left(\mu_0 - \frac{u_0^2}{4\varkappa}\right) + i\zeta_n\mu_1^{2/3}\varkappa^{1/3} = \omega_s(0) + i\zeta_n\mu_1^{2/3}\varkappa^{1/3}, \quad n \in \mathbb{N}. \tag{4.9}$$

Thus, the condition of growth of the nth global eigenmode $\mathrm{Im}\omega_n^g > 0$ is equivalent to the condition

$$\mathrm{Im}\,\omega_s(0) > |\zeta_n|\mu_1^{2/3}\,\mathrm{Re}\,\varkappa^{1/3}, \tag{4.10}$$

i.e., the increment of local absolute instability of the initial velocity profile must be greater than the value of the right-hand side of the resulting inequality, which, in turn, depends on the decrease rate of this increment downstream μ_1. This condition connects the local properties of absolute instability and the global instability of flow evolving downstream. Since the zero $\zeta_1 \approx -2.338$ of the Airy function is the smallest in absolute value, the condition of global instability can be rewritten in the form:

$$\mathrm{Im}\,\omega_s(0) > |\zeta_1|\mu_1^{2/3}\,\mathrm{Re}\,\varkappa^{1/3}. \tag{4.11}$$

The global eigenmodes of model equation (4.6) take the form:

$$A_n(x,t) = e^{i\omega_n^g t}e^{i\alpha_s x}\mathrm{Ai}\left(\left(\frac{\mu_1}{\varkappa}\right)^{1/3}\left(x + \zeta_n\left(\frac{\varkappa}{\mu_1}\right)^{1/3}\right)\right). \tag{4.12}$$

We will consider the spatial eigenmode distribution, which is the product of two functions of the spatial coordinate. Obviously, the first multiplier $e^{i\alpha_s x}$ describes spatial oscillations with the wavenumber of the local saddle point α_s, which correspond to the asymptotics of the localized disturbance in the plane-parallel approximation. In other words, these oscillations correspond to local absolute instability of flow. The second multiplier $\mathrm{Ai}((\mu_1/\varkappa)^{1/3}(x + \zeta_n(\varkappa/\mu_1)^{1/3}))$ describes the envelope that ensures the fulfillment of the damping conditions at $x = 0$ and as $x \to +\infty$, the characteristic wavelength of the envelope being associated with the parameter μ_1 that characterizes the decrease rate of the absolute instability increment (4.5). The slower the spatial evolution of the unperturbed flow, the smaller μ_1, that is, the smaller the difference between the global natural frequency and the absolute instability frequency $\omega_s(0)$ in the initial jet cross-section, the more extended the eigenfunction becomes in space. Thus, the resulting solution (4.12) describes modes arising from local absolute instability occurring in a finite spatial interval.

4.3. An Example of the Globally Unstable Jet

Above, in Section 3, we carried out calculations of the evolution of plane submerged jets. We will now show that the characteristics of absolute instability can be sufficient for the development of global instability of an evolving jet. In what follows, an initial velocity profile with the parameters $\xi = 0.1$ and $\zeta = 1.6$ is taken for analysis. In Fig. 6 we have reproduced its downstream evolution, as well as the location of the inflection point on the profile. It can be noted that the increase in the velocity at the inflection point in the initial stages of jet development occurs very rapidly. This is caused by the large curvature of the profile at the edge of jet, but slows down downstream as the velocity profile "spreads out" and its curvature decreases.

In Fig. 7 we have reproduced the mapping of curves $\mathrm{Im}\omega = \mathrm{Im}\omega_s(x)$ into the complex plane α for several velocity profiles corresponding to several coordinates x of the developing jet. As can be seen, the location of the saddle point depends only slightly on x: the relative change in $\mathrm{Re}\alpha_s$ is equal to 2% and the relative changes in $\mathrm{Im}\,\alpha_s$ and $\mathrm{Re}\,\omega_s = 10\%$. The orientation of the branches $\alpha(\omega)$ approaching the saddle point, determined by $\mathrm{Arg}\lambda$, changes more significantly, but $\mathrm{Arg}\lambda$ relates to the quantity θ in (2.8) and does not determine the asymptotic behavior of localized perturbations in the plane-parallel case. The quantity $|\lambda|$, which determines the asymptotics (2.8) due to connection $|\omega''(\alpha_s)| = 2/|\lambda|$ (4.2), varies only slightly - within 3%. These considerations make it possible to accept coefficients (4.4) to be close to constants.

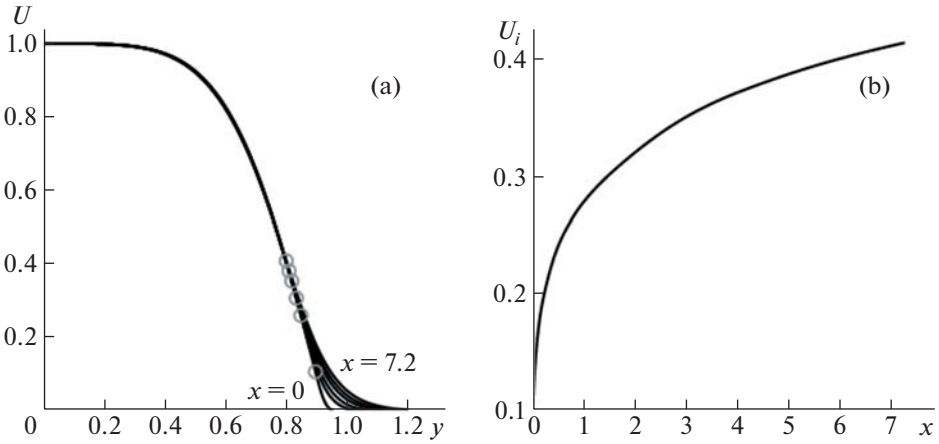

Fig. 6. Velocity profiles at $x = 0.0$, 0.8, 1.8, 3.4, 5.0, and 7.2 for the initial profile corresponding to $\xi = 0.1$, $\zeta = 1.6$, circles show the location of the inflection point (a). Velocity at the inflection point of the velocity profile as a function of the streamwise coordinate x (b).

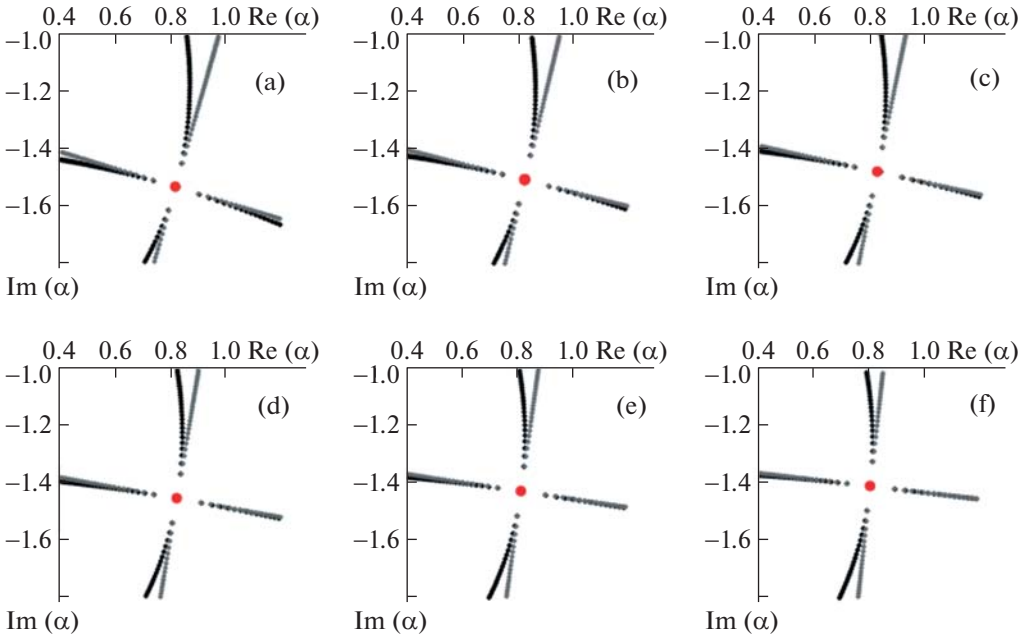

Fig. 7. Mapping of a curve $\mathrm{Im}\,\omega = \mathrm{Im}\,\omega_s$ into the plane α for a jet profile corresponding to the distances $x = 0$ (a), 0.8 (b), 1.8 (c), 3.4 (d), 5.0 (e), and 7.2 (f) from the initial cross-section. The calculation based on the Rayleigh equation is shown by black color, the approximation (4.2) with the parameters of Table 1 is shown by gray color, circle shows the saddle point $\alpha = \alpha_s$.

In Table 1 we have given the found values of $\alpha_s(x)$, $\omega_s(x)$, and $\lambda(x)$. The corresponding parameters $\varkappa$ and u_0 are presented in Table. 2.

In Fig. 8 we have plotted the graph of variation in $\mathrm{Im}\,\omega_s(x)$. From the graph it is obvious that the decrease in the growth rate of absolute instability is approximately linear. Taking this fact into account, the parameter μ_1 can be estimated from Table 1 as follows:

$$\mu_1 = -\frac{d\,\mathrm{Im}\,\omega}{dx} \approx 0.00700.$$

Taking the zero of the Airy function with the smallest absolute value $\zeta_1 \approx -2.338$ and considering various $\varkappa$ from Table 2, we obtain the following estimates for the right-hand side of (4.11): 0.042; 0.043;

Table 1. Saddle-point parameters at varios distances from inlet

x	α_s	ω_s	λ
0.0	$0.820 - 1.535i$	$0.927 + 0.050i$	$2.993 - 1.932i$
0.8	$0.827 - 1.503i$	$0.911 + 0.041i$	$3.212 - 1.693i$
1.8	$0.827 - 1.479i$	$0.897 + 0.032i$	$3.343 - 1.488i$
3.4	$0.824 - 1.450i$	$0.879 + 0.021i$	$3.452 - 1.237i$
5.0	$0.819 - 1.428i$	$0.863 + 0.011i$	$3.510 - 1.038i$
7.2	$0.808 - 1.405i$	$0.845 + 0.000i$	$3.546 - 0.815i$

Table 2. Estimates of the parameters of Eq. (4.6) at various distances from inlet

x	$\varkappa$	u_0
0.0	$-0.152 + 0.236i$	$-0.854 + 0.475i$
0.8	$-0.128 + 0.244i$	$-0.789 + 0.520i$
1.8	$-0.111 + 0.250i$	$-0.741 + 0.555i$
3.4	$-0.092 + 0.257i$	$-0.690 + 0.593i$
5.0	$-0.077 + 0.262i$	$-0.650 + 0.622i$
7.2	$-0.062 + 0.268i$	$-0.606 + 0.653i$

0.044; 0.045; 0.045; and 0.046 at $x = 0.0$, 0.8, 1.8, 3.4, 5.0, and 7.2, respectively. Condition (4.8) is satisfied in all cases. Since $\mathrm{Im}\,\omega_s(0) = 0.050$, global instability condition (4.11) is satisfied for all five velocity profiles. Taking into account the approximate nature of estimate of the parameter $\varkappa$, we can expect the presence of global instability, that is, in this case, local absolute instability in a limited spatial interval is fairly strong to generate global instability.

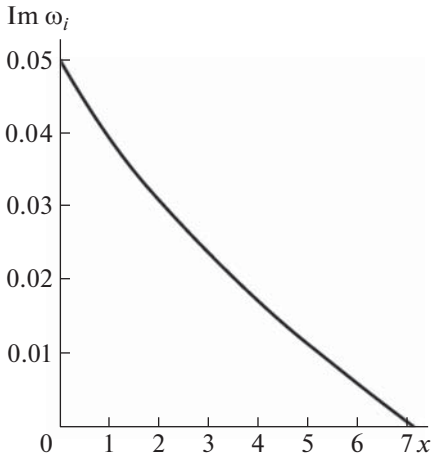

Fig. 8. Increment of local absolute instability $\mathrm{Im}\omega_s$ as a function of the longitudinal coordinate x.

SUMMARY

An algorithm that determines the length of the region of local absolute instability of a submerged jet with a given initial velocity profile has been developed. After parameterizing the initial velocity profile, its evolution downstream is calculated, then the nature of instability of the velocity profiles at various distances from the beginning of the resulting jet is analyzed. The nature of instability is determined by the behavior of the level lines $\mathrm{Im}\,\omega = 0$ of the frequency ω on the complex plane of the wavenumber α. In the studied class of the initial velocity profiles, a domain of parameters for which the largest length of the region of local absolute instability of the jet $L \approx 7.6$ is realized was found.

The presence of a fairly extended region of local absolute instability of the flow leads to its global instability [12, 13]. To determine the quantitative characteristics of local instability, which would lead to global instability, based on consideration of the model equation, a relation between the characteristics of local absolute instability (which occurs in a limited spatial interval) and the global natural frequencies and modes is obtained. The initial velocity profile of a jet from the class of profiles under consideration, for which the existence of the growing global eigenmode is expected, is demonstrated. Thus, the possibility of existence of the global instability of a plane submerged jet evolving in space is shown.

The experimental implementation of a globally unstable submerged jet can be carried out using the technology described in [25]. This problem is of both fundamental and applied interest: such a flow can be used to accelerate transition to turbulence in various technical devices and intensify mixing, for example, in nozzles of combustion chambers and in chemical reactors.

FUNDING

The work was supported by the Russian Science Foundation Grant no. 20-19-00404-P.

CONFLICT OF INTEREST

The authors of this work declare that they have no conflicts of interest.

REFERENCES

1. Zaiko, Yu.S., Reshmin, A.I., Teplovodskii, S.Kh., and Chicherina, A.D., Investigation of submerged jets with an extended initial laminar region, *Fluid Dyn.*, 2018, vol. 53, no. 1, pp. 95–104.
2. Zayko, J., Teplovodskii, S., Chicherina, A., Vedeneev, V., and Reshmin, A., Formation of free round jets with long laminar regions at large Reynolds numbers, *Phys. Fluids,* 2018, vol. 30, p. 043603.
3. Zayko, J.S., Gareev, L.R., Chicherina, A.D., Trifonov, V.V., Vedeneev, V.V., and Reshmin, A.I., Experimental Validation of Linear-Stability Theory Applied to a Submerged Jet, *Dokl. Phys.*, 2021, vol. 66, pp. 106–109.
4. Gareev, L.R., Zayko, J.S., Chicherina, A.D., Trifonov, V.V., Reshmin, A.I., and Vedeneev, V.V., Experimental validation of inviscid linear stability theory applied to an axisymmetric jet, *J. Fluid Mech.*, 2022, vol. 934, no. A3.
5. Schlichting, H., *Boundary Layer Theory*, McGraw-Hill, 1979.
6. Iordanskii, S.V. and Kulikovskii, A.G., The absolute stability of some plane-parallel flows at high Reynolds numbers, *Soviet Physics JETP*, 1966, vol. 22, no. 4, pp. 915–918.
7. Deissler, R.L., The convective nature of instability in plane Poiseuille flow, *Phys. Fluids,* 1987, vol. 30, no. 8, pp. 2303–2305.
8. Brevdo, L., Convectively unstable wave packets in Blasius boundary layer, *ZAMM,* 1995, vol. 75, no. 6, pp. 423–436.
9. Abid, M., Brachet, M., and Huerre, P., Linear hydrodynamic instability of circular jets with thin shear layers, *Eur. J. Mech. B/Fluids,* 1993, vol. 12(5), pp. 683–693.
10. Vedeneev, V.V. and Zayko, J.S., On absolute stability of free jets, *J. Phys: Conf. Series,* 2018, vol. 1129, p. 012037.
11. Vedeneev, V. and Nikitin, N., Absolute instability of plane incompressible jets, *J. Fluid Mech.*, 2023, vol. 962, no. A4.
12. Chomaz, J.-M., Huerre, P., Redekopp, L.G., A frequency selection criterion in spatially developing flows, *Stud. Appl. Math.*, 1991, vol. 84, no. 2, pp. 119–144.
13. Le Dizes, S., Huerre, P., Chomaz, J.M., Monkewitz, P.A., Linear global modes in spatially developing media, *Philos. Trans. R. Soc. London A,* 1996, vol. 354, no. 1705, pp. 169–212.
14. Monkewitz, P.A., The absolute and convective nature of instability in two-dimensional wakes at low Reynolds numbers, *Phys. Fluids*, 1988, vol. 31, no. 5, pp. 999–1006.
15. Pier, B., On the frequency selection of finite-amplitude vortex shedding in the cylinder wake, *J. Fluid Mech.*, 2002, vol. 458, pp. 407–417.

16. Coenen, W., Lesshafft, L., Garnaud, X., and Sevilla, A., Global instability of low-density jets, *J. Fluid Mech.*, 2017, vol. 820, pp. 187–207.
17. Woodley, B.M. and Peake, N., Global linear stability analysis of thin aerofoil wakes, *J. Fluid Mech.*, 1997, vol. 339, pp. 239–260.
18. Le Dizés, S., Global modes in falling capillary jets, *Eur. J. Mech., B/Fluids*, 1997, vol. 16, no. 6, pp. 761–778.
19. Yakubenko, P.A., Global capillary instability of an inclined jet, *J. Fluid Mech.*, 1997, vol. 346, pp. 181–200.
20. Vedeneev, V.V., Poroshina, A.B. Stability of an Elastic Tube Conveying a Non-Newtonian Fluid and Having a Locally Weakened Section, *Proc. Steklov Inst. Math.*, 2018, vol. 300, pp. 34–55.
21. Bondarev, V. and Vedeneev, V., Short-wave instability of an elastic plate in supersonic flow in the presence of the boundary layer, *J. Fluid Mech.*, 2016, vol. 802, pp. 528–552.
22. Vedeneev, V.V., *Matematicheskaya teoriya ustoihivosti ploskoparallel'nykh techenii i razvitie turbulentnosti* (Mathematical Theory of Stability of Plane-Parallel Flows and the Development of Turbulence: Textbook), Dolgoprudnyi: Intellekt, 2016. (in Russian).
23. Couairon, A. and Chomaz, J.-M., Fully nonlinear global modes in slowly varying flows, *Phys. Fluids,* 1999, vol. 11, no. 12, pp. 3688–3703.
24. Lavrentyev, M.A. and Shabat, B.V., *Metody teorii funktsii kompleksnogo peremennogo* (Methods of the Theory of Functions of a Complex Variable), Moscow: Nauka, 1965. (in Russian).
25. Spasova, A.A., Zayko, J.S., Development of an algorithm for generating a submerged jet with specified velocity profile characteristics, *J. Appl. Mech. Tech. Phys.*, 2023, vol. 64, pp. 610–617.

Translated by E.A. Pushkar